Novel Tricyclic Inhibitors of IκB Kinase

James Kempson,*,† Steven H. Spergel,† Junqing Guo,† Claude Quesnelle,† Patrice Gill,† Dominique Belanger,† Alaric J. Dyckman,† Tianle Li,† Scott H. Watterson,† Charles M. Langevine,† Jagabandhu Das,† Robert V. Moquin,† Joseph A. Furch,† Anne Marinier,† Marco Dodier,† Alain Martel,† David Nirschl,¶ Katy Van Kirk,¶ James R. Burke,‡ Mark A. Pattoli,‡ Kathleen Gillooly,‡ Kim W. McIntyre,‡ Laishun Chen,§ Zheng Yang,§ Punit H. Marathe,§ David Wang-Iverson,§ John H. Dodd,† Murray McKinnon,‡ Joel C. Barrish,† and William J. Pitts†

Departments of Discovery Chemistry, Discovery Biology, and Metabolism and Pharmacokinetics and Synthesis and Analysis Technology Team, Bristol-Myers Squibb Research and Development, P.O. Box 4000, Princeton, New Jersey, 08543-4000

Received December 15, 2008

The design and synthesis of a novel series of oxazole-, thiazole-, and imidazole-based inhibitors of IκB kinase (IKK) are reported. Biological activity was improved compared to the pyrazolopurine lead, and the expedient synthesis of the new tricyclic systems allowed for efficient exploration of structure−activity relationships. This, combined with an iterative rat cassette dosing strategy, was used to identify compounds with improved pharmacokinetic (PK) profiles to advance for in vivo evaluation.

Introduction

The nuclear transcription factor NF-κB[a] has a crucial role in the pathogenesis of several human disorders, particularly those with an inflammatory component.[1] In unstimulated cells, NF-κB is sequestered in the cytoplasm as an inactive complex with IκB inhibitory protein.[2] In the case of IκBα, the most extensively studied member of this protein family, the stimulation of proinflammatory receptors such as the tumor necrosis factor (TNF) receptor, activates the so-called "canonical" pathway of NF-κB activation in which a multisubunit IKK complex catalyzes the phosphorylation of IκBα at Ser32 and Ser36.[3] This phosphorylation event is essential for signaling the subsequent ubiquitination and proteosomal degradation of IκBα, thus leaving the NF-κB free to translocate to the nucleus and activate proinflammatory gene transcription.

The IKK complex comprises two catalytic subunits, IKK1 and IKK2 (also termed IKKα and IKKβ, respectively). Although both of these subunits can catalyze the phosphorylation of IκB protein, evidence has shown that the IKK2 subunit plays a major role in NF-κB activation arising from proinflammatory stimuli such as TNF-α, IL1-β, IL-6, IL-17, and IL-23.[4] Since IKK2 is vital for translating these proinflammatory stimuli into the activation of NF-κB, an inhibitor of IKK2 could be effective in the treatment of autoimmune and inflammatory disorders such as rheumatoid arthritis, inflammatory bowel disease, lupus, and multiple sclerosis. Interestingly, the activity of glucocorticoids, which are among the most effective anti-inflammatory agents available, is mediated primarily through the inhibition of NF-κB mediated transcription. This suggests that an IKK2 inhibitor would provide an opportunity to develop novel therapeutics that has the potential for glucocorticoid-like activity but without their trans-activation related toxicities.[5]

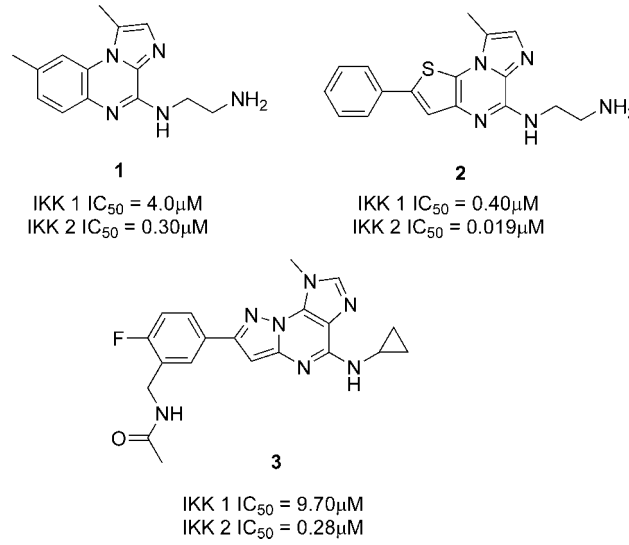

Figure 1. Previous IKK inhibitors discovered at Bristol-Myers Squibb.

The discovery of small molecule IKK inhibitors as orally active therapeutic agents for the treatment of inflammatory diseases has been the goal of numerous research groups, and several classes of IKK inhibitors have been reported.[6] We recently reported the identification of the imidazoquinoxaline based inhibitor of IKK2, **1** (Figure 1).[6b] Despite promising in vivo efficacy studies in both acute and chronic preclinical models of inflammation, the compound has relatively weak in vitro potency which prompted a search for alternative inhibitors of IKK2 with greater potency. Discovery of the thiophene[6e] and pyrazolopurine[6f] chemotypes followed by structure−activity relationship (SAR) modification led to the identification of **2** and **3** as potent and selective inhibitors of IKK2. Both of these chemotypes, however, were metabolically unstable resulting in poor PK profiles, and their lengthy chemical syntheses drasti-

* To whom correspondence should be addressed. Phone: (609) 252-4539. Fax: (609) 252-7410. E-mail: james.kempson@bms.com.
† Department of Discovery Chemistry.
¶ Synthesis and Analysis Technology Team.
‡ Department of Discovery Biology.
§ Department of Metabolism and Pharmacokinetics.

[a] Abbreviations: IKK, IκB kinase; TNF, tumor necrosis factor; IL, interleukin; NF-κB, nuclear factor κ light-chain enhancer of activated B cells; ser, serine; SAR, structure−activity relationship; PK, pharmacokinetic; GST, glutathione *s*-transferase; LPS, lipopolysaccharide; PBMC, peripheral blood mononuclear cell; AUC, area under curve; V_{ss}, volume of distribution; CYP, cytochrome P450.

10.1021/jm8015816 CCC: $40.75
Published on Web 03/06/2009

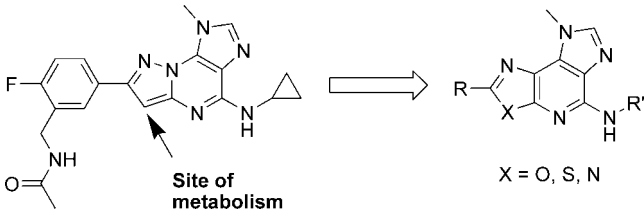

Figure 2. Metabolism driven design of new IKK inhibitors.

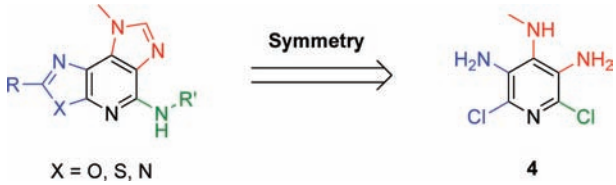

Figure 3. Disconnection of newly proposed IKK targets to common intermediate.

Scheme 1[a]

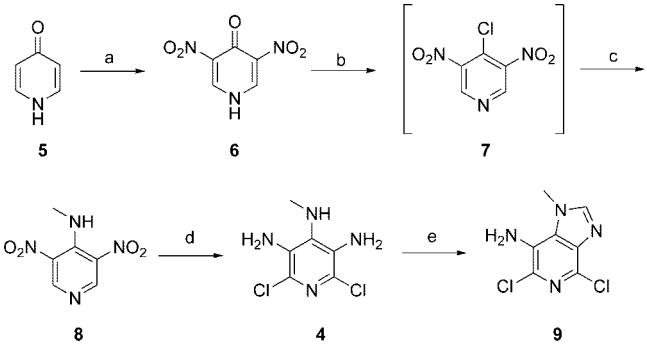

[a] Conditions: (a) fuming HNO_3, conc H_2SO_4, reflux, 85%; (b) $POCl_3$, PCl_5, reflux; (c) 2.0 M $MeNH_2$ in THF, 0 °C, 65% for two steps; (d) $SnCl_2$, conc HCl, 100 °C, 50−60%; (e) $CH(OEt)_3$, CH_3CN, 100 °C, 95%.

cally slowed SAR generation, with no opportunity for chemotype diversification.

Design of New Tricyclic Based Inhibitors of IKK

Metabolite identification of the pyrazolopurine and thiophene-based tricyclic chemotypes revealed core oxidation as a major metabolic pathway. New isosteric tricyclic chemotypes were designed to block the current site of metabolism, leading to compounds of the type shown in Figure 2.

Disconnection from these newly proposed tricycle targets led to the novel C_s-symmetrical pentasubstituted pyridine intermediate **4** (see Figure 3). It was anticipated that this common intermediate could be used to access the desired chemotypes as well as facilitate a more rapid SAR analysis than was previously possible. This approach was particularly attractive, since there was no IKK2 protein structure to guide our efforts, and as such, an efficient chemotype construction/SAR modification strategy was of paramount importance.

Chemistry

The synthesis of the C_s-symmetrical pyridine, **4**, and its conversion to the common intermediate, **9**, is outlined in Scheme 1. Nitration of commercially available 4-hydroxypyridine, **5**, was carried out according to literature methods to afford **6**.[7] Treatment of **6** with PCl_5 in phosphorus oxychloride gave the unstable intermediate **7**. Attempts to isolate this compound resulted in significant hydrolysis back to **6**, hence **7** was treated directly with methylamine to give **8**. The reduction of each nitro

Scheme 2[a]

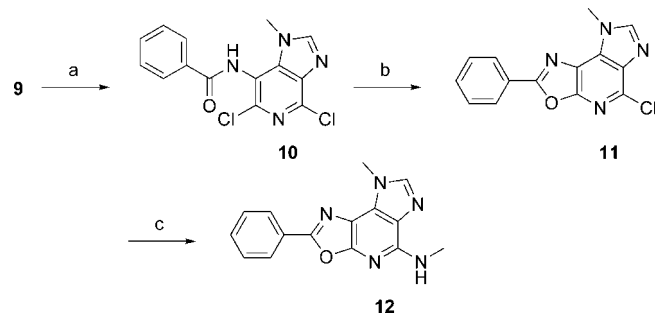

[a] Conditions: (a) benzoyl chloride, CH_2Cl_2, room temp, 100%; (b) Na_2CO_3, DMF, microwave, 220 °C, 60%; (c) $MeNH_2 \cdot HCl$, $(i\text{-Pr})_2NEt$, *n*-BuOH, 140 °C, 40%.

Scheme 3[a]

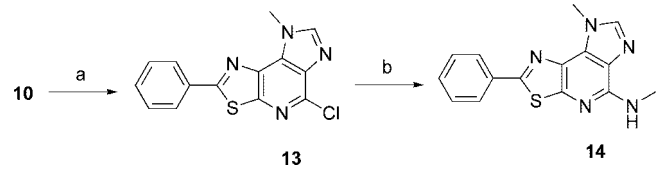

[a] Conditions: (a) Lawesson's reagent, toluene, 110 °C, then K_2CO_3, DMA, 160 °C, 75%; (b) $MeNH_2 \cdot HCl$, $(i\text{-Pr})_2NEt$, *n*-BuOH, 140 °C, 33%.

Scheme 4[a]

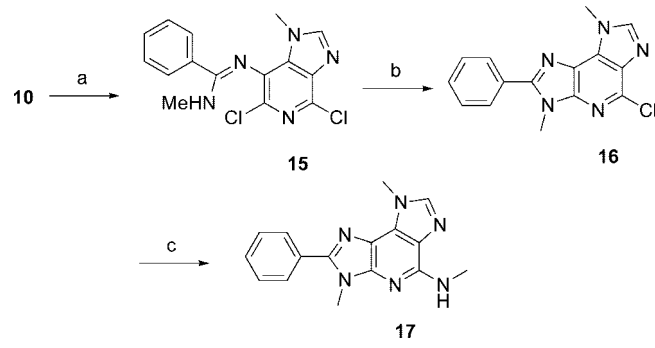

[a] Conditions: (a) (i) $SOCl_2$, toluene, 110 °C; (ii) $MeNH_2 \cdot HCl$, $(i\text{-Pr})_2NEt$, CH_3CN, 80 °C, (83% for two steps); (b) KO^{t}Bu, DMF, microwave, 200 °C, 67%; (c) $MeNH_2 \cdot HCl$, $(i\text{-Pr})_2NEt$, *n*-BuOH, 185 °C, 18%.

group with concomitant installation of the chlorine groups at the 2- and 6-positions of the pyridine ring was accomplished in a single step by treatment with tin(II) chloride.[8] Desymmetrization was then accomplished by the reaction of **4** with 1 equivalent of triethyl orthoformate to give **9**.

Schemes 2−4 outline the synthesis of the oxazole, thiazole, and imidazole tricyclic cores, **12**, **14**, and **17**, respectively. In the oxazole case, common intermediate **9** was treated with 1 equiv of benzoyl chloride. The resulting amide, **10**, was isolated as the hydrochloride salt and then cyclized in the presence of sodium carbonate in DMF at 220 °C under microwave irradiation to give **11**. Displacement of the 2-chloropyridine in **11** was then achieved with methylamine and led to the first oxazole-based compound **12**. The structure of **12** was confirmed by X-ray crystallographic analysis of the HCl salt. Amide **10** was also treated with Lawesson's reagent (see Scheme 3), which after base-induced cyclization led to the thiazole **13**. In a manner similar to the oxazole case, final displacement with methylamine then provided the first thiazole-based tricycle **14**, whose structure was also confirmed by X-ray crystallographic analysis. Scheme 4 depicts the synthesis of a third tricyclic core, which was

Scheme 5[a]

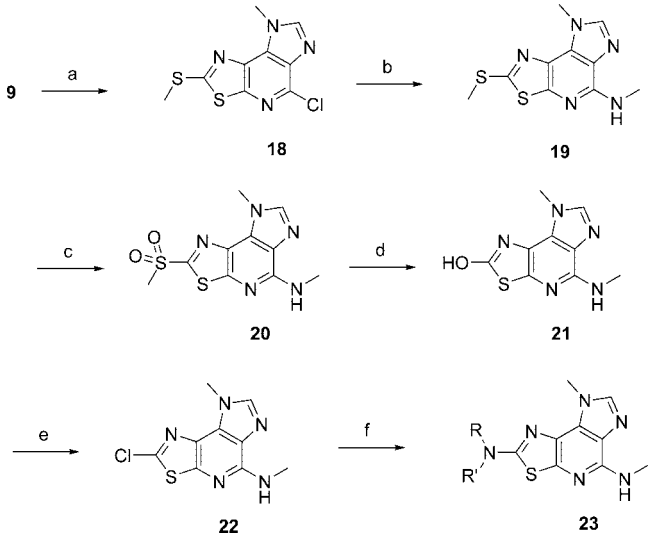

[a] Conditions: (a) Ppotassium thioxanthate, MeI, DMF, 55%; (b) $MeNH_2$ in EtOH, *n*-BuOH, 180 °C, 91%; (c) Oxone, CH_2Cl_2; (d) 5 N NaOH, 48% (for two steps); (e) $POCl_3$, pyridine, 180 °C, 90%; (d) RR′NH, K_2CO_3, NMP, 140 °C, 30−75%.

Scheme 6[a]

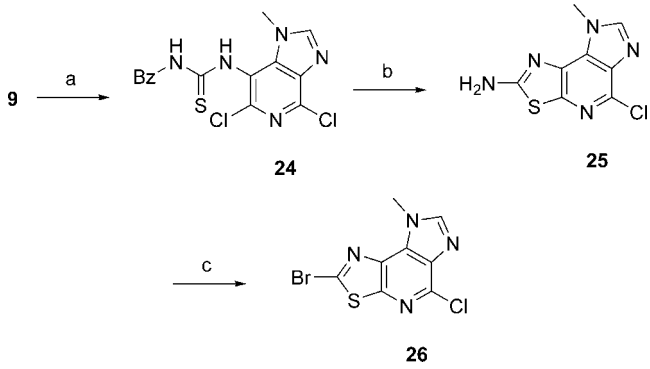

[a] Conditions: (a) BzNCS, acetone, 75%; (b) (i) KO^{t}Bu, NMP; (ii) HCl, dioxane, 64%; (c) isoamylnitrile, $CuBr_2$, CH_3CN, 82%.

achieved via conversion of amide **10** into the corresponding chloroimidate with thionyl chloride and subsequent displacement with methylamine to provide **15**. Closure with potassium *tert*-butoxide gave **16**, which after final displacement with methylamine resulted in **17**.

Scheme 5 highlights the initial synthetic approach to generate increased diversity in the thiazole chemotype. Reaction of **9** with potassium thioxanthate followed by in situ alkylation with methyl iodide afforded **18** in 55% yield. Displacement with methylamine under microwave conditions then provided **19**. The structure was confirmed by X-ray crystallographic analysis (see Supporting Information). Oxidation to the sulfone **20** with oxone followed by hydrolysis to **21** and subsequent chlorination using phosphorus oxychloride provided the advanced intermediate **22**. Displacement with a variety of amines provided compounds **23**.

Scheme 6 highlights a complementary synthetic approach to the thiazole tricyclic system, again starting from the common intermediate, **9**. Condensation of **9** with benzoylisothiocyanate gives **24**. This undergoes cyclization and amide cleavage to give the 2-aminothiazole **25**. Sandmeyer reaction in the presence of isoamyl nitrite and copper bromide then provides **26**. This advanced intermediate proved more efficient for the SAR investigations that were conducted in this series.

Scheme 7[a]

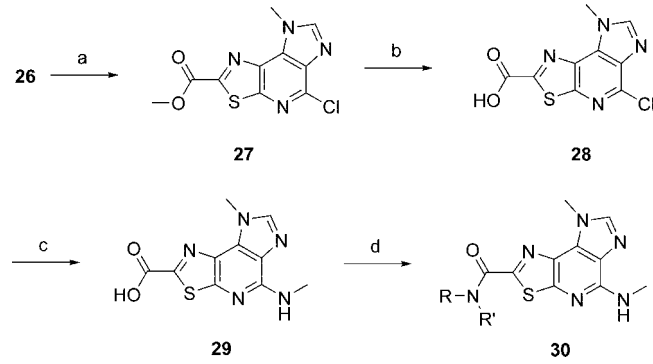

[a] Conditions: (a) $PdCl_2(PPh_3)_2$, Et_3N, 1:1 CH_3CN/MeOH, 100 psi CO, 60 °C, 91%; (b) NaOH, THF, 53%; (c) $MeNH_2$ in EtOH, 150 °C, 36%; (d) RR′NH, PyBOP, NMP, 52−83%.

Scheme 8[a]

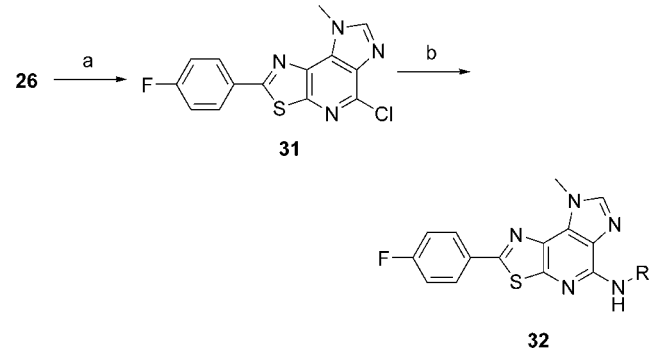

[a] Conditions: (a) 4-fluorophenylboronic acid, K_2CO_3, $Pd(PPh_3)_4$, 1:1 DME/EtOH, 100 °C, 60%; (b) RNH_2 in EtOH, 150 °C, 22−64%.

Scheme 9[a]

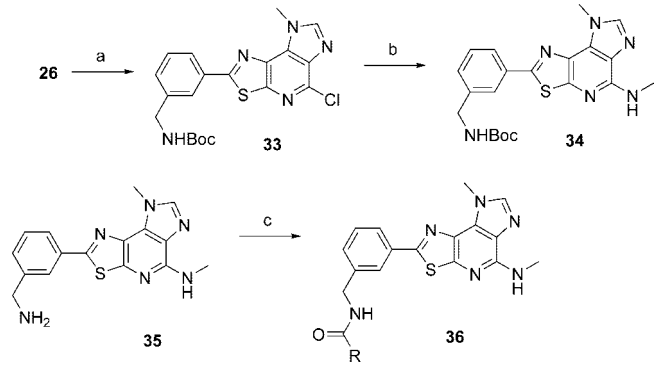

[a] Conditions: (a) 3-(*N*-Boc-aminomethyl)phenylboronic acid, K_2CO_3, $Pd(PPh_3)_4$, 1:1 DME/EtOH, 100 °C, 60%; (b) RNH_2 in EtOH, 150 °C, 10−75%; (c) HCl in dioxane, 80%; (d) RCO_2H, PyBOP, NMP, 36−85%.

Carbonylation of the bromo intermediate **26** provided the ester **27**, which after hydrolysis furnished the carboxylic acid **28** (Scheme 7). Displacement with methylamine then gave **29**, which proved useful to probe structural diversity via amide couplings employing pyBOP and an amine to give **30**.

Scheme 8 highlights a Suzuki coupling with 4-fluorophenylboronic acid to give **31**. This compound then formed the basis for SAR exploration at the 2-position of the pyridine ring. Chemistry described previously using a variety of amines was used to generate the desired inhibitors **32**.

Suzuki coupling reaction with 3-(*N*-Boc-aminomethyl)phenylboronic acid (Scheme 9) followed by nucleophilic displacement with methylamine and subsequent acid deprotection of

Table 1. Enzyme, Cell Activities, and in Vitro Metabolic Stabilities for Program "Lead" **3b** and New Oxazole, Thiazole, and Imidazole Tricycles **12**, **14**, and **17**, Respectively

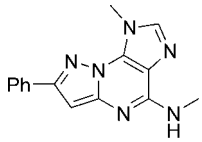

3b

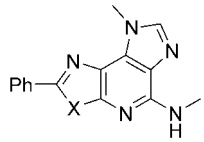

12 X = O
14 X = S
17 X = NMe

compd	IKK-1 IC_{50}, μM	IKK-2 IC_{50}, μM	PBMC IC_{50}, μM	microsomal clearance in rat, human, mouse, nmol/(min·mg)
3b	0.99	0.034	0.47	0.05, 0.11, 0.17
12	0.27	0.011	0.39	0.14, 0.09, 0.23
14	3.5	0.006	0.31	0.12, 0.09, 0.25
17	4.3	0.52	0.44	0.08, 0.13, 0.12

the Boc group gave **35**. This then allowed for derivatization at the benzylamine, providing **36** with a variety of carboxylic acids.

Results and Discussion

Compounds were evaluated for their ability to inhibit IKK1 or IKK2 catalyzed phosphorylation of glutathione *s*-transferase (GST)−IκBα fusion protein, and a peripheral blood mononuclear cell assay (PBMC) was used to measure the ability of compounds to inhibit lipopolysaccharide (LPS)-induced TNFα production in human primary cells.

By use of the previously outlined syntheses (Schemes 1−4), the oxazole, thiazole, and imidazole tricycles **12**, **14**, and **17** were initially prepared to test the concept of blocking metabolism. Both the oxazole **12** and thiazole **14** displayed improved enzyme activites with IKK2 IC_{50} values of 0.011 and 0.006 μM, respectively (Table 1), compared to 0.034 μM for the pyrazolopurine **37** (3- to 6-fold increase in potency). Cellular (PBMC) activities were also improved, although not to the same extent as the enzyme potencies. Interestingly, the thiazole tricycle also displayed a marked increase in IKK1/IKK2 selectivity (580-fold). Although **12**, **14**, and **17** are isosteric, **17** proved to be somewhat less potent than the other two tricyclic systems.

Encouraged by the improvements in enzyme and cell activities for two of the three newly synthesized chemotypes, their metabolic stability in rat, human, and mouse liver microsomes was then evaluated in in vitro assays. Disappointingly, both the oxazole and thiazole chemotypes displayed the same moderate-to-poor metabolic profiles, with negligible improvement in human liver microsome stability compared to the pyrazolopurine **3b** and even worse profiles in mouse and rat. Clearance rates for the imidazole **17** were comparable to **3b** across all three species. Although the microsomal stability profiles were less than ideal, the potent thiazole analogue and the pyrazolopurine **3b** were further evaluated in rats dosed with an intravenous (2 mg/kg) administration of compound in order to determine their clearance rate (Table 2). For the pyrazolopurine, **3b**, in vivo clearance was higher than predicted by incubation with liver microsomes. Despite the apparent increase in in vitro microsomal degradation of **14** compared with **3b**, in vivo pharmacokinetic evaluation in rats showed a minor improvement in clearance (Table 2).

Although the concept of blocking metabolism had resulted in minor improvements to in vivo clearance in the case of **14**, over the course of our studies it became apparent that the in vitro metabolic stability assay had little predictive value with respect to the metabolism of the tricycle (thiazole) core. In an attempt to address this issue, we implemented a cassette screening strategy in which we simultaneously administered five compounds at a dose of 2 mg/kg.[9] In an effort to exclude false positives resulting from drug interactions, compounds were prescreened in cytochrome P450 (CYP) assays to exclude potent inhibitors ($IC_{50} < 10$ μM). The thiazole chemotype was selected not only because of its potent and selective inhibition of IKK2 but also because of the amount of chemical diversity we could explore in this chemotype arising from the same intermediate. A focused library effort would allow efficient modification at the 2- and 6-positions of the thiazole core (see Figure 4). The linear synthesis of previous tricyclic systems had thus far limited the 6-position SAR to aryl and heteroaryl groups. Expansion of this to include amine and amide functionality was planned for the first time. It was hoped that this strategy, after iterative cassette screening, would identify compounds that maintained the potency of **14** *and* had favorable PK profiles.

Table 2. Rat Pharmacokinetic Data for Compounds **3b** and **14**

compd	C_{max},[a] nM	AUC, nM·h	$T_{1/2}$, h	clearance, (mL/min)/kg	V_{ss}, L/kg
3b	3600	2200	0.5	55	2.1
14	3000	2800	1.2	42	2.8

[a] Maximum serum concentration after intravenous (2 mg/kg) administration of the compound to rat in Tween 80: H_2O (1:9) medium; $n = 3$ animals

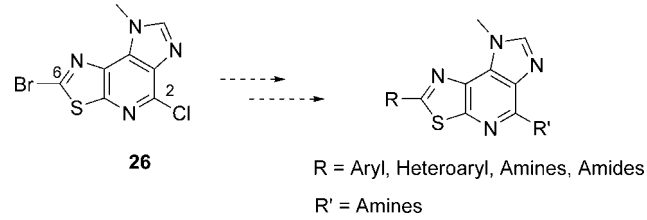

26

R = Aryl, Heteroaryl, Amines, Amides
R' = Amines

Figure 4. SAR strategy from new common intermediate **26**.

Schemes 5−9 highlight the implementation of the SAR strategy that began with amine modification at the 6-position of the thiazole core. Despite encouraging results with the thiomethyl and sulfone (**19** and **20**, respectively) analogues, subsequent substitution studies with a variety of amines revealed a narrow structural requirement at this position. Replacement of the thiomethyl substituent with primary amines significantly attenuated potency. Examination of cyclic compounds **23d**, **23e**, and **23f** suggested that enzyme potency could be optimized to some extent but cell activity, as with all analogues in this class, remained weak (Table 3).

Our attention turned next to the modification of the carboxamide substituent on the thiazole core (Table 4). Both the Me and Et amide analogues (**30a** and **30b**) are equipotent against IKK2. Replacement with cyclopentylamide **30c** leads to a substantial loss (10-fold) in potency which is further attenuated with the tertiary di-Et amide **30d**. The thienylamide **30e** displays the same enzyme potency as **30a** and **30b**, although again for this series of compounds cellular potency is generally weak.

Table 5 summarizes the 2-aminopyridine SAR which was conducted with a *p*-fluorophenyl group at the 6-position. SAR findings in related series restricted this effort to primary amines, since removal of the N−H bond donor resulted in a drastic loss of enzyme potency. All amines studied maintained a modest amount of activity against IKK2. Although the amine and alcohol functionality of **32a**−**f** were tolerated by the enzyme, **32e** and **32f** possessed significant cytotoxicity as measured by an Alamar blue toxicity assay.[10] This is possibly due to the

Table 3. Enzyme and Cell Activities for Thiazole Tricycles Derived from Scheme *5*

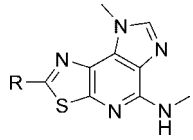

compd	R	IKK-1 IC_{50}, μM	IKK-2 IC_{50}, μM	PBMC[a] IC_{50}, μM
19		2.6	0.028	0.58
20		7.6	0.081	3.3
23a		3.4	0.92	2.6
23b	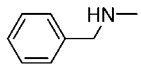	NT[b]	1.5	NT[b]
23c	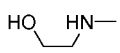	NT[b]	0.30	NT[b]
23d		8.1	0.033	0.85
23e		6.1	0.21	0.66
23f	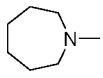	NT[b]	0.13	0.45

[a] PBMC = LPS induced TNF-α production in peripheral blood mononuclear cells. [b] NT = not tested.

detergent-like nature of the molecules bearing a polar "head" group and a lipophilic *p*-fluorophenyl "tail".

Efforts then turned to the meta-position of the phenyl ring which in previous efforts had proved successful, allowing modulation of both enzyme and cell potencies as well as physicochemical characteristics. Table 6 summarizes the SAR findings. Addition of *m*-benzylamine derivatives maintained reasonable potency (compounds **37a**, **37b**). Removal of the *p*-fluoro group led to significantly improved enzyme and cellular activities. Sulfonamide **36b** in particular represented the most potent inhibitor studied. Further benzylamine derivatization led to heterocyclic amides **36c** and **36d** which, despite a 3- to 5-fold drop in enzyme potency, still maintained similar potency in cellular assays to **36b**.

Given the initial SAR findings, we next wanted to investigate the impact of each of these structural modifications on the in vivo clearance of the compounds. Consistent with all aminothiazoles tested, **23f** displayed high in vitro microsomal clearance which translated into high clearance (83 (mL/min)/kg) and low exposure in rats (Table 7). Improvements seen with the amide **30d** were quickly abolished with the first phenyl analogue **32a** which highlights the lack of correlation between the in vitro system and in vivo clearance. Amine modifications **32d** and **32e** led to significant (Cl = 16 (mL/min)/kg) and slight (52 (mL/min)/kg) improvements, respectively, compared to **32a** (67 (mL/min)/kg). Meta-substitution significantly improved clearance over **32a**, while removal of the *p*-fluoro group led to an increase in in vivo clearance. Optimization of the amides gave

Table 4. Enzyme and Cell Activities for Thiazole Tricycles Derived from Scheme *7*

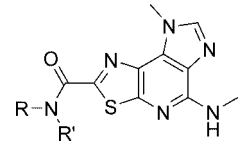

compd	R	IKK-1 IC_{50}, μM	IKK-2 IC_{50}, μM	PBMC[a] IC_{50}, μM
30a		0.84	0.015	0.97
30b		1.1	0.015	1.7
30c	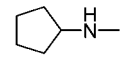	NT[b]	0.16	NT[b]
30d		20	2.5	3.5
30e	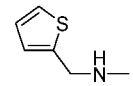	NT[b]	0.015	0.63

[a] PBMC = LPS induced TNF-α production in peripheral blood mononuclear cells. [b] NT = not tested.

Table 5. Enzyme Activities and Cytotoxicity Data for Thiazole Tricycles Derived from Scheme *8*

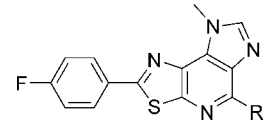

compd	R	IKK-1 IC_{50}, μM	IKK-2 IC_{50}, μM	% Viability @ 100 μM
32a		3.1	0.026	74.
32b		3.4	0.039	86
32c		>20	0.18	NT[a]
32d	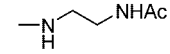	5.0	0.033	80
32e	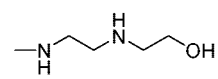	8.6	0.075	0.0
32f	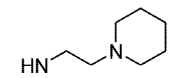	8.3	0.056	0.0

[a] NT = not tested.

Table 6. Enzyme and Cell Activities for Thiazole Tricycles Derived from Scheme *9*

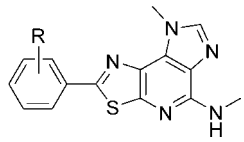

compd	R	IKK-1 IC_{50}, μM	IKK-2 IC_{50}, μM	PBMC[a] IC_{50}, μM
37a	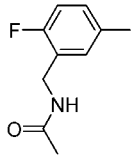	3.5	0.053	NT[b]
37b	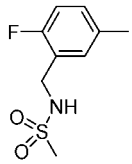	4.2	0.032	NT[b]
36a	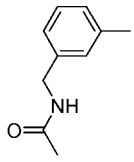	1.9	0.022	0.35
36b	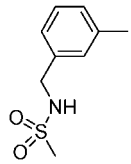	1.0	0.005	0.16
36c	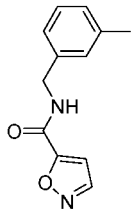	1.4	0.025	0.17
36d	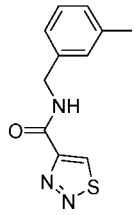	10	0.016	0.082

[a] PBMC = LPS induced TNF-α production in peripheral blood mononuclear cells. [b] NT = not tested.

36c and **36d** which represented the most improved compounds with respect to both IKK2 and PBMC potency as well as metabolic stability.

The in vivo activity of the thiazole tricyclic based IKK inhibitors was demonstrated by assessment of **36d** in an acute murine model of TNFα production. Mice were dosed orally with **36d** at 10 mg/kg, 4 h prior to LPS administration, and TNFα levels were measured 90 min later. As shown in Figure 5, **36d** is orally active with statistically significant (50%) reduction in serum TNF compared to vehicle control.

Table 7. In Vitro and in Vivo Clearance Data for Different Structural Elements in the Thiazole Chemotype

compd	microsomal clearance in rat, human, mouse, nmol/(min·mg)	C_{max},[a] nM	AUC, nM·h	$T_{1/2}$, h	clearance, (mL/min)/kg	V_{ss}, L/kg
23f	0.25, 0.15, 0.29	300	250	0.4	83	2.6
30d	NT[b]	1100	880	1.2	23	0.6
32a	0.095, 0.13, 0.21	1600	1600	0.6	67	3.2
32d	0.000, 0.003, 0.065	4700	2700	0.4	16	0.5
32e	0.000, 0.000, 0.000	600	590	2.6	52	10.4
37a	NT[b]	800	570	0.3	31	0.5
37b	0.12, 0.030, 0.14	1200	800	0.4	20	0.4
36b	0.13, 0.015, 0.16	500	400	0.3	41	0.9
36c	0.16, 0.18, 0.26	2300	1900	0.4	8.4	0.2
36d	0.14, 0.16, 0.23	3900	5000	0.6	3.0	0.2

[a] Maximum serum concentration after intravenous (2 mg/kg) administration of the compound to rat in Tween-80/H_2O (1:9) medium; $n = 3$ animals. [b] NT = not tested.

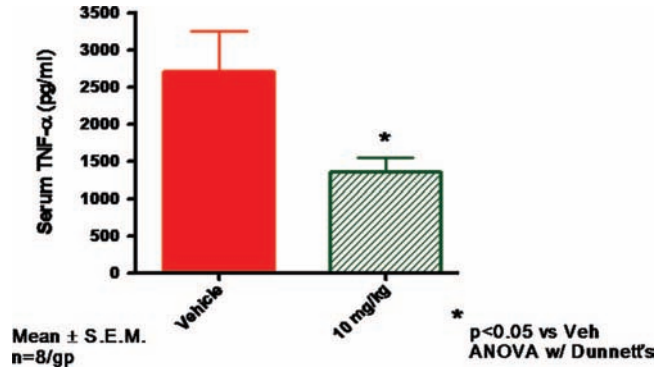

Figure 5. LPS-induced TNF inhibition by **36d** in mice. BALB/c female mice (Harlan), 6−8 weeks of age, were used. Compound was dissolved in poly(ethylene glycol) (MW = 300, PEG300) and administered to mice ($n = 8$/treatment) by oral gavage in a volume of 0.1 mL. Control mice received PEG300 alone ("Veh"). Four hours later, mice were injected intraperitoneally with 50 μg/kg lipopolysacchride (LPS, *E. coli* O111:B4; Sigma). Blood samples were collected 90 min after LPS injection. Serum was separated and analyzed for the level of TNF-α by commercial ELISA assay (BioSource) according to the manufacturer's instruction. Data shown are the mean ± SEM.

Table 8. Kinase Selectivity Profile for Compounds **12**, **17**, and **36a**[a]

compd	IKK2	Btk	Cdk2	IGF	Itk	IKKε	Plk1	Src
12	0.011	23	16	<50	17	17	<50	<50
17	0.52	14	23	<50	19	14	12	<50
36a	0.022	17	31	<50	9.1	12	<50	<50

[a] Enzyme inhibition in μM.

Representative examples of each tricyclic core were evaluated in an in-house kinase selectivity panel ($n = 30$), and in general, the compounds were found to possess a high degree of selectivity (Table 8).

Conclusion

In an attempt to improve the low metabolic stability of the pyrazolopurine and thiophene tricycles, we developed a new synthetic route to block the proposed common site of metabolism in these molecules. Novel oxazole, thiazole, and imidazole tricycles were prepared to test this hypothesis. The oxazole and thiazole displayed improved potency against IKK2; however, these parent compounds still suffered from poor PK. The expedient nature of the synthetic route allowed for significant diversification via a common intermediate, and this, in combination with a cassette screening strategy, was successful in

identifying compounds with improved PK. When dosed orally at 10 mg/kg, **36d** inhibited LPS-induced TNF-α production in mice. Efforts continue to optimize this and other series and will be reported in the future.

Experimental Section

Proton magnetic resonance (^{1}H) spectra were recorded on either a Bruker Avance 400 or a JEOL Eclipse 500 spectrometer and are reported in ppm relative to the reference solvent of the sample in which they were run. HPLC and LCMS analyses were conducted using a Shimadzu SCL-10A liquid chromatograph and a SPD UV−vis detector at 220 or 254 nm with the MS detection performed with either a Micromass Platform LC spectrometer or a Waters Micromass ZQ spectrometer. Preparative reverse-phase HPLC purifications were performed using the following conditions: Ballistic YMC S5 ODS 20 mm × 100 mm column with a binary solvent system, where solvent A is 10% methanol, 90% water, 0.1% trifluoroacetic acid and solvent B is 90% methanol, 10% water, and 0.1% trifluoroacetic acid; flow rate of 20 mL/min; linear gradient time of 10 min; start %B = 20; final %B = 100. Fractions containing the product were concentrated in vacuo to remove the methanol and were neutralized with aqueous sodium bicarbonate. The products were collected by vacuum filtration or were extracted with organic solvents and concentrated under reduced pressure. All flash column chromatography was performed on EM Science silica gel 60 (particle size of 40−60 μm). All reagents were purchased from commercial sources and used without further purification unless otherwise noted. All reactions were performed under an inert atmosphere. Microwave reactions were performed using a Personal Chemistry SmithSynthesizer workstation with a power range of 300 W provided from a magnetron at 2.45 GHz. The purity of all tested compounds was determined by HPLC (see HPLC Methods below) and were ≥95% pure.

HPLC Methods. HPLC analyses were performed using the following conditions.

Method A. A linear gradient program using 10% MeOH−90% H_2O−0.1% TFA (solvent A) and 90% MeOH−10% H_2O−0.1% TFA (solvent B); t = 0 min, 0% B, t = 2 min, 100% B; was employed on a YMC ODS-A S7 C28 3.0 mm × 50 mm column. Flow rate was 5 mL/min, and UV detection was set to 254 nm. The LC column was maintained at ambient temperature.

Method B. A linear gradient program using 10% MeOH−90% H_2O−0.2% H_3PO_4 (solvent A) and 90% MeOH−10% H_2O−0.2% H_3PO_4 (solvent B); t = 0 min, 0% B, t = 4 min, 100% B; was employed on a YMC ODS-A S7 C28 3.0 mm × 50 mm column. Flow rate was 4 mL/min, and UV detection was set to 254 nm. The LC column was maintained at ambient temperature.

Method C. A linear gradient program using 5% acetonitrile−95% H_2O−0.05% TFA (solvent A) and 95% acetonitrile−5% H_2O−0.05% TFA (solvent B); t = 0 min, 10% B, t = 25 min, 100% B; was employed on a SunFire C18 3.5 μm, 4.6 mm × 150 mm column. Flow rate was 1 mL/min, and UV detection was set to 254 nm. The LC column was maintained at ambient temperature.

Method D. A linear gradient program using 5% acetonitrile−95% H_2O−0.05% TFA (solvent A) and 95% acetonitrile−5% H_2O−0.05% TFA (solvent B); t = 0 min, 10% B, t = 25 min, 100% B; was employed on a XBridge phenyl 3.5 μm, 4.6 mm × 150 mm column. Flow rate was 1 mL/min, and UV detection was set to 254 nm. The LC column was maintained at ambient temperature.

(3,5-Dinitropyridin-4-yl)methylamine (8). 6 (10.0 g, 0.051 mol) was added portionwise to a mixture of phosphorus oxychloride (25 mL) and PCl_5 (17.0 g, 0.082 mol). The reaction mixture was heated to reflux under a nitrogen atmosphere for 12 h. The reaction mixture was allowed to cool to room temperature and the phosphorus oxychloride removed in vacuo. The residue was suspended in dry THF (50 mL) and cooled to 0 °C. Methylamine (32 mL, 2.0 M in THF, 0.064 mol) was added dropwise over 20 min under a nitrogen atmosphere, and the resulting solution was allowed to warm to room temperature over 1 h. The reaction mixture was evaporated in vacuo and the residue suspended in ethyl acetate (200 mL) which was then filtered and the filtrate evaporated in vacuo to produce the crude product. The crude product was recrystallized from methanol (100 mL) to give **8** as a tan solid (7.2 g, 71% for two steps). ^{1}H NMR ($CDCl_3$) δ 9.06 (s, 1H), 8.84 (s, 1H), 2.98 (s, 3H). MS (ESI) m/z 199 $(M + H)^+$. Purity: 98% (method A, t_R = 1.58 min).

2,6-Dichloro-*N*′-methylpyridine-3,4,5-triamine (4). A solution of **8** (60.0 g, 0.30 mol) in concentrated hydrochloric acid (300 mL) was heated to 90 °C. Tin(II) chloride (85.0 g, 0.45 mol) was added portionwise over 1 h with vigorous effervescence noted for the first equivalent of tin chloride added. The reaction mixture was heated for a further hour before the additon of more tin chloride (28.0 g, 0.15mol) and continued heating for 2 more hours. The reaction mixture was cooled to 0 °C and cautiously basified with concentrated ammonium hydroxide (200 mL). The precipitated solid was filtered off and the filtrate extracted with ethyl acetate (5 × 200 mL). The combined organics were dried ($MgSO_4$) and evaporated in vacuo to produce **4** as a brown solid (28.0 g, 46%). ^{1}H NMR (DMSO-d_6) δ 4.94 (br s, 5H), 2.60 (s, 3H). ^{13}C NMR (DMSO-d_6) δ 133.9, 130.7, 121.6, 31.9. MS (ESI) m/z 207 $(M + H)^+$. Purity: 97% (method A, t_R = 0.71 min), 98% (method B, t_R = 1.20 min).

7-Amino-4,6-dichloro-1-methyl-1*H*-imidazo[4,5-*c*]pyridine (9). Triethyl orthoformate (25.0 mL, 0.15mol) was added in one portion to a suspension of **4** (28 g, 0.14mol) in dry acetonitrile (400 mL). The reaction mixture was heated to reflux for 4 h and then cooled to room temperature. The reaction mixture was evaporated in vacuo to produce **9** as a brown powder. ^{1}H NMR (DMSO-d_6) δ 8.20 (1H, s), 5.49 (2H, br s), 4.07 (3H, s). MS (ESI) m/z 217 $(M + H)^+$. Purity: 98% (method A, t_R = 0.78 min).

***N*-(4,6-Dichloro-1-methyl-1*H*-imidazole[4,5-*c*]pyridin-7-yl)-benzamide (10).** Benzoyl chloride (1.2 g, 10.1 mmol) in dry acetonitrile (100 mL) was added in one portion to a suspension of the amine **9** (2.0 g, 9.2 mmol), and the resulting mixture was heated to 70 °C for 6 h. The reaction mixture was concentrated in vacuo to produce the crude product which was precipitated with methanol and filtered to give **7** (1.3 g, 44%). ^{1}H NMR (DMSO-d_6) δ: 8.30 (1H, s), 8.20 (2H, app d, J = 1.0 Hz), 7.87 (2H, app t, J = 6.0 Hz), 7.70 (2H, app t, J = 8.0 Hz), 5.55 (1H, s), 4.15 (3H, s). MS (ESI) m/z 321 $(M + H)^+$. Purity: 98% (method A, t_R = 1.20 min).

7-Chloro-4-methyl-2-phenyl-4*H*-imidazo[4,5-*d*]oxazolo[5,4-*b*]-pyridine (11). Sodium carbonate (0.35 g, 3.3mmol) was added in one portion to a solution of **10** (0.96 g, 3.0 mmol) in *N*,*N*-dimethylformamide (30 mL), and the reaction mixture was heated to 160 °C for 24 h. The reaction mixture was cooled to room temperature and evaporated in vacuo. The residue was partitioned between dichloromethane (50 mL) and water (50 mL). The separated organic layer was dried ($MgSO_4$) and evaporated in vacuo to produce the oxazole **11** (0.42 g, 49%). ^{1}H NMR (DMSO-d_6) δ 8.34 (1H, s), 8.05 (2H, dd, J = 6.0 Hz, 1.0 Hz), 7.50−7.45 (3H, m), 4.02 (3H, s). MS (ESI) m/z 285 $(M + H)^+$. Purity: 98% (method A, t_R = 1.74 min), 100% (method B, t_R = 3.43 min).

4-Methyl-7-methylamino-2-phenyl-4*H*-imidazo[4,5-*d*]oxazolo[5,4-*b*]pyridine (12). Methylamine hydrochloride (104 mg, 1.54 mmol) and diisopropylethylamine (0.54 mL, 3.08mmol) were each added in one portion to a suspension of **11** (200 mg, 0.7 mmol) in *n*-butanol (1 mL). The reaction mixture was heated in the microwave at 180 °C for 4 h. The reaction mixture was evaporated in vacuo and the residue suspended between ethyl acetate (5 mL) and water (5 mL). The separated organic layer was dried ($MgSO_4$) and evaporated in vacuo to leave the crude product which was purified by preparative HPLC (reverse phase) to produce **12** (38 mg, 19%). ^{1}H NMR (DMSO-d_6) δ 8.20 (1H, s), 8.07−7.98 (2H, m), 7.49−7.38 (3H, m), 4.83 (3H, s), 4.08 (3H, s). HRMS for $C_{15}H_{14}O_1N_5$ $(M + H)^+$, calcd: 280.1193. Found: 280.1191. Purity: 100% (method C, t_R = 12.57 min), 100% (method D, t_R = 10.97 min).

7-Chloro-4-methyl-2-phenyl-4*H*-imidazo[4,5-*d*]thiazolo[5,4-*b*]-pyridine (13). A mixture of **10** (43 mg, 0.13 mmol) and Lawesson's reagent (80 mg, 0.2 mmol) in toluene (2 mL) was heated to 110 °C for 5 h. After the mixture was cooled to room temperature, 1,8-diazabicyclo[5.4.0]undec-7-ene (0.06 mL, 0.4 mmol) was added

and the reaction mixture was allowed to stir for 60 h. The volatiles were removed in vacuo, and the residue was dissolved in *N*,*N*-dimethylacetamide (2 mL). After adding potassium carbonate (50 mg, 0.36 mmol), the reaction mixture was heated to 160 °C for 1 h. The reaction mixture was cooled to room temperature and partitioned between ethyl acetate (20 mL) and water (20 mL). After washing with water (2 × 20 mL) and brine (20 mL), the organic layer was dried ($MgSO_4$). Filtration and concentration afforded a crude residue that was purified by preparative thin layer chromatography (20 cm × 20 cm, 1 mm thick silica gel plate) using ethyl acetate as the eluent. Extraction of the desired band with ethyl acetate, filtration, and concentration afforded 21 mg (75%) of **13** as an off-white solid. ^{1}H NMR (DMSO-d_6) δ 8.52 (1H, s), 8.15−8.12 (2H, m), 7.65−7.58 (3H, m), 4.30 (3H, s). MS (ESI) *m*/*z* 301 $(M + H)^+$. Purity: 93% (method A, t_R = 1.89 min), 92% (method B, t_R = 3.73 min).

4-Methyl-7-methylamino-2-phenyl-4*H*-imidazo[4,5-*d*]thiazolo[5,4-*b*]pyridine (14). A mixture of **13** (19 mg, 0.063 mmol), methylamine hydrochloride (22 mg, 0.32 mmol), and diisopropylethylamine (0.092 mL, 0.5 mmol) in 0.5 mL of *n*-butanol was heated to 180 °C for 4.5 h in a sealed tube, using a microwave apparatus. After cooling to room temperature, the reaction mixture was partitioned between ethyl acetate (20 mL) and saturated sodium bicarbonate solution (20 mL). The aqueous layer was extracted with ethyl acetate (20 mL), and the combined organic layers were dried ($MgSO_4$). Filtration and concentration afforded a residue that was triturated with ethyl ether and dried to afford 6 mg (33%) of **14** as a yellow powder. ^{1}H NMR (DMSO-d_6) δ 8.20 (1 H, s), 8.01 (1 H, d, J = 6.80 Hz), 7.42−7.60 (3 H, m), 4.22 (3 H, s), 3.00 (3 H, s). HRMS for $C_{15}H_{14}N_5S_1$ $(M + H)^+$, calcd: 296.0964. Found: 296.0956. Purity: 100% (method C, t_R = 11.12 min), 95% (method D, t_R = 10.73 min).

***N*-(4,6-Dichloro-1-methyl-1*H*-imidazo[4,5-*c*]pyridin-7-yl)-*N*′-methylbenzamidine (15). 10** (2.65 g, 8.3mmol) was suspended in toluene (100 mL) and thionyl chloride (1.97 g, 16.6mmol) added in one portion. The resulting mixture was refluxed for 24 h before cooling to room temperature and evaporating in vacuo. The resulting tan solid was washed with diethyl ether (100 mL) and dried under vacuum to afford 2.8 g of a solid that was immediately used in the next reaction.

The tan solid (1.0 g, 2.9mmol) was added in one portion to a mixture of methylamine hydrochloride (398 mg, 5.9 mmol) and *N*,*N*-diisopropylethylamine (760 mg, 5.9mmol) in acetonitrile (100 mL). The resulting mixture was refluxed for 48 h before cooling and evaporating in vacuo. The residue was then partitioned between dichloromethane (50 mL) and saturated sodium bicarbonate solution (75 mL). The organic layer was then dried ($MgSO_4$) and evaporated in vacuo. The residue was triturated with diethyl ether (100 mL) to afford 0.8 g (83%) of **15** as a white powder. ^{1}H NMR (DMSO-d_6) δ 8.30 (1 H, s), 7.70−7.92 (2 H, m), 7.12−7.38 (3 H, m), 4.02 (3 H, s), 2.94 (3 H, d, J = 3.27 Hz). HRMS for $C_{15}H_{14}N_5Cl_2$ $(M + H)^+$, calcd: 334.062 08. Found: 334.061 54. Purity: 95% (method B, t_R = 1.25 min).

7-Chloro-1,4-dimethyl-2-phenyl-4*H*-imidazo[4,5-*d*]imidazo[5,4-*b*]pyridine (16). Potassium *tert*-butoxide (200 mg, 1.8mmol) was added in one portion to a solution of **15** (300 mg, 0.9mmol) in DMF (2.0 mL), and the resulting solution was heated in the microwave at 200 °C for 1 h. The solvent was then removed in vacuo and the residue taken up in 95:5 dichloromethane/methanol (50 mL). This organic layer was then washed with water (2 × 50 mL), and the separated organic layer was then dried ($MgSO_4$) and evaporated in vacuo. The residue was then triturated with diethyl ether (50 mL) to afford 179 mg (67%) of **16** as a tan solid. ^{1}H NMR (DMSO-d_6) δ 8.36 (1 H, s), 7.93 (1 H, dd, J = 7.55, 2.01 Hz), 7.51−7.71 (4 H, m), 4.21 (3 H, s), 3.97 (3 H, s). HRMS for $C_{15}H_{13}N_5Cl_1$ $(M + H)^+$, calcd: 298.085 40. Found: 298.084 85. Purity: 95% (method B, t_R = 2.84 min).

1,4-Dimethyl-7-methylamino-2-phenyl-4*H*-imidazo[4,5-*d*]imidazo[5,4-*b*]pyridine (17). 16 (700 mg, 2.4mmol) was added in one portion to a mixture of methylamine hydrochloride (700 mg, 10.3 mmol) and *N*,*N*-diisopropylethylamine (1.4 g, 10.8mmol) in *n*-butanol (3 mL). The resulting mixture was heated in the microwave at 185 °C for 4 h. The reaction mixture was then evaporated in vacuo and purified by preparative HPLC to afford 124 mg (18%) of **17** as a yellow solid. ^{1}H NMR (DMSO-d_6) δ 8.15 (1 H, s), 7.83−7.93 (1 H, m), 7.54−7.68 (4 H, m), 4.12 (3 H, s), 3.92 (3 H, s), 3.03 (3 H, s). HRMS for $C_{16}H_{17}N_6$ $(M + H)^+$, calcd: 293.150 92. Found: 293.150 39. Purity: 97% (method C, t_R = 6.62 min), 95% (method D, t_R = 8.14 min).

7-Chloro-4-methyl-2-(methylthio)-4*H*-imidazo[4,5-*d*]thiazolo[5,4-*b*]pyridine (18). 9 (2.17 g, 10 mmol) and potassium thioxanthate (3.05 g, 20mmol) were added to 20 mL of DMF and heated for 2.5 h at 145 °C. The reaction mixture was cooled to room temperature and then placed in an ice bath and cooled to ∼0 °C. Methyl iodide (1.24 mL, 20 mmol) was added and the reaction mixture stirred for 1 h in the ice bath. Volatile liquids were removed at ∼45 °C under high vacuum. The residue was partitioned between chloroform (150 mL) and saturated sodium bicarbonate (100 mL). The aqueous layer was washed with additional chloroform (2 × 75 mL). The combined organic layers were dried over magnesium sulfate, filtered, and evaporated to provide a cream-colored solid. The crude product was triturated with hot ethyl acetate (∼75 mL) which was allowed to cool to room temperature. The product was collected by filtration, and 1.49 g (55%) of **18** was isolated as a cream-colored solid. ^{1}H NMR (DMSO-d_6) δ 8.48 (1 H, s), 4.20 (3 H, s), 2.86 (3 H, s). HRMS for $C_9H_8N_4Cl_1S_2$ $(M + H)^+$, calcd: 270.9873. Found: 270.9872. Purity: 88% (method A, t_R = 1.58 min), 92% (method B, t_R = 3.06 min).

4-Methyl-7-methylamino-2-(methylthio)-4*H*-imidazo[4,5-*d*]thiazolo[5,4-*b*]pyridine (19). 18 (540 mg, 2 mmol) and 1.5 mL of methylamine in ethyl alcohol (12 mmol) was added to *n*-butanol (5 mL) and heated to 180 °C in a sealed tube for 4 h and cooled to room temperature. HPLC indicated that the reaction had not proceeded to completion. Additional methylamine in ethyl alcohol (12 mmol) was added and the reaction vessel sealed and heated for an additional 4 h. The reaction mixture was cooled to room temperature and the volatile solvent removed under vacuum. The residue was triturated with water and the residue dried under high vacuum to provide 428 mg (91%) of **19** as a white powder. ^{1}H NMR (DMSO-d_6) δ 8.09 (1 H, s), 7.13 (1 H, d, J = 4.78 Hz), 4.11 (3 H, s), 2.94 (3 H, d, J = 4.78 Hz), 2.75 (3 H, s). HRMS for $C_{10}H_{12}N_5S_2$ $(M + H)^+$, calcd: 266.0529. Found: 266.0526. Purity: 99% (method C, t_R = 7.50 min), 100% (method D, t_R = 7.64 min).

2-Methanesulfonyl-4-methyl-7-methylamino-4*H*-imidazo[4,5-*d*]-thiazolo[5,4-*b*]pyridine (20). To a stirred mixture of **19** (5.22 g, 19.6 mmol) in MeOH (80 mL) was added a suspension of Oxone (35 g) in H_2O (80 mL). After 3 h, the mixture was partially concentrated, diluted with H_2O, neutralized with $NaHCO_3$ and then the solid was collected by filtration to provide 3.22 g (55%) of **20**. ^{1}H NMR (DMSO-d_6) δ 8.23 (1 H, s), 7.83 (1 H, d, J = 4.78 Hz), 4.15 (3 H, s), 3.49 (3 H, s), 3.00 (3 H, d, J = 4.53 Hz). HRMS for $C_{10}H_{12}O_2N_5S_2$ $(M + H)^+$, calcd: 298.0427. Found: 298.0423. Purity: 100% (method C, t_R = 8.15 min), 95% (method D, t_R = 7.63 min).

2-Hydroxy-4-methyl-7-methylamino-4*H*-imidazo[4,5-*d*]thiazolo[5,4-*b*]pyridine (21). To **20** (3.22 g) as a suspension in H_2O (25 mL) was added 5 N NaOH, and the resulting mixture was heated to 120 °C for 3 h. The mixture was then allowed to cool to room temperature before acidifying with 20 mL AcOH and the resulting solid was collected by filtration to afford 2.22 g (48%) of **21** as a tan solid. MS (ESI) *m*/*z* 236 $(M + H)^+$. Purity: 95% (method A, t_R = 1.58 min).

2-Chloro-4-methyl-7-methylamino-4*H*-imidazo[4,5-*d*]thiazolo[5,4-*b*]pyridine (22). A mixture of **21** (1.00 g, 4.25 mmol) and pyridine (0.35 mL) in $POCl_3$ (20 mL) was heated to 140 °C with stirring for 48 h. The mixture was cooled to room temperature and concentrated. The residue was partitioned between 1% H_2SO_4 and $CHCl_3$, and the aqueous phase was separated and extracted with THF (2×). The combined organic phases were dried ($MgSO_4$), filtered, and concentrated to dryness. The residue was triturated with $CHCl_3$/EtOAc 1:10 to provide 975 mg (90%) **22** as a beige solid. MS (ESI) *m*/*z* 254 $(M + H)^+$. Purity: 98% (method A, t_R = 1.76 min).

4-Methyl-7-methylamino-2-methylamino-4*H*-imidazo[4,5-*d*]thiazolo[5,4-*b*]pyridine (23a). To a solution of **22** (10 mg, 0.039 mmol) in NMP (0.5 mL) was added a solution of methylamine (1 mL of a 0.5 M solution in NMP) and K_2CO_3 (10 mg) and then heated to 140 °C overnight. The mixture was cooled to room temperature, and AcOH (0.50 mL) was added, filtered, and purified directly by preparative HPLC to afford 3.3 mg (28%) of **23a** as a film. ^{1}H NMR (DMSO-d_6) δ 7.96 (1 H, s), 7.55 (1 H, d, J = 4.78 Hz), 6.49 (1 H, d, J = 4.78 Hz), 4.06 (3 H, s), 3.33 (6 H, s). HRMS for $C_{10}H_{13}N_6S_1$ $(M + H)^+$, calcd: 249.0917. Found: 249.0914. Purity: 95% (method C, t_R = 4.12 min), 100% (method D, t_R = 4.63 min).

4-Methyl-7-methylamino-2-benzylamino-4*H*-imidazo[4,5-*d*]thiazolo[5,4-*b*]pyridine (23b). 23b was prepared as a pale-yellow solid following the procedure described for **23a**. ^{1}H NMR (DMSO-d_6) δ 8.10 (1 H, s), 7.34−7.40 (4 H, m), 7.13−7.17 (1 H, m), 4.63 (2 H, s), 4.15 (3 H, s), 3.00 (3 H, d, J = 4.53 Hz). HRMS for $C_{16}H_{16}N_6S_1$ $(M + H)^+$, calcd: 324.1157. Found: 327.1148. Purity: 100% (method C, t_R = 8.15 min), 95% (method D, t_R = 7.63 min).

4-Methyl-7-methylamino-2-hydroxyethylamino-4*H*-imidazo[4,5-*d*]thiazolo[5,4-*b*]pyridine (23c). 23c was prepared as a pale-yellow solid following the procedure described for **23a**. ^{1}H NMR (DMSO-d_6) δ 7.95 (1 H, s), 7.49−7.74 (1 H, m), 6.38−6.55 (1 H, m), 4.78 (1 H, t, J = 5.29 Hz), 4.07−4.16 (2 H, m), 4.04 (3 H, s), 3.59 (2 H, q, J = 5.71 Hz), 3.16 (3 H, s). HRMS for $C_{11}H_{15}O_1N_6S_1$ $(M + H)^+$, calcd: 279.1023. Found: 279.1023. Purity: 95% (method C, t_R = 3.28 min), 100% (method D, t_R = 3.60 min).

4-Methyl-7-methylamino-2-[1,2,3,6-tetrahydropyridine]-4*H*-imidazo[4,5-*d*]thiazolo[5,4-*b*]pyridine (23d). 23d was prepared as a pale-yellow solid following the procedure described for **23a**. ^{1}H NMR (DMSO-d_6) δ 7.99 (1 H, s), 6.55−6.72 (1 H, m), 5.70−6.00 (2 H, m), 4.04−4.20 (5 H, m), 3.98 (2 H, d, J = 2.27 Hz), 3.64 (2 H, t, J = 5.67 Hz), 3.20 (3 H, s). HRMS for $C_{14}H_{17}N_6S_1$ $(M + H)^+$, calcd: 301.1230. Found: 301.1230. Purity: 100% (method C, t_R = 7.79 min), 100% (method D, t_R = 9.05 min).

4-Methyl-7-methylamino-2-piperidine-4*H*-imidazo[4,5-*d*]thiazolo[5,4-*b*]pyridine (23e). 23e was prepared as a pale-yellow solid following the procedure described for **23a**. ^{1}H NMR (DMSO-d_6) δ 8.05 (1 H, s), 4.15 (3 H, s), 3.56−3.60 (4 H, m), 3.10 (3 H, s), 1.66−1.77 (6 H, m). HRMS for $C_{14}H_{18}N_4S_1$ $(M + H)^+$, calcd: 302.1314. Found: 302.1310. Purity: 100% (method C, t_R = 8.15 min), 95% (method D, t_R = 7.63 min).

4-Methyl-7-methylamino-2-(azepan-1-yl)-4*H*-imidazo[4,5-*d*]thiazolo[5,4-*b*]pyridine (23f). 23f was prepared as a pale-yellow solid following the procedure described for **23a**. ^{1}H NMR (DMSO-d_6) δ 8.23 (1 H, s), 7.83 (1 H, d, J = 4.78 Hz), 4.15 (3 H, s), 3.49 (6 H, s), 3.33 (6 H, s), 3.00 (3 H, d, J = 4.53 Hz). HRMS for $C_{15}H_{21}N_6S_1$ $(M + H)^+$, calcd: 317.1543. Found: 317.1542. Purity: 97% (method C, t_R = 9.03 min), 97% (method D, t_R = 10.50 min).

1-Benzoyl-3-(4,6-dichloro-1-methyl-1*H*-imidazo[4,5-*c*]pyridine-7-yl)thiourea (24). 9 (6.94 g, 31.0 mmol) was suspended in acetone (120 mL). Benzoyl isothiocyanate (5.8 g, 35 mmol) was added dropwise over 10 min, and the reaction mixture was allowed to stir at room temperature overnight before heating to reflux for 1 h. The reaction mixture was then cooled to room temperature and the solvent removed under reduced pressure. Ethyl alcohol (50 mL) was added to the solid and the mixture heated to reflux for 1 h, then cooled to room temperature and allowed to stand for several hours. The product was collected by filtration and dried under vacuum to afford 11.32 g (93%) of **24** as a white powder. ^{1}H NMR (DMSO-d_6) δ 12.18 (1H, s), 12.10 (1H, s), 8.48 (1H, s), 8.10−8.06 (2H, m), 7.70−7.65 (1H, m), 7.59−7.55 (2H, m), 4.26 (3H, s). MS (ESI) m/z 380, 382 $(M + H)^+$. Purity: 98% (method A, t_R = 2.10 min).

7-Chloro-4-methyl-2-amino-4*H*-imidazo[4,5-*d*]thiazolo[5,4-*b*]pyridine (25). Potassium *tert*-butoxide (1 M solution in THF, 24 mL, 24 mmol) was evaporated to dryness under reduced pressure and the residue dissolved in NMP 15 mL). **24** (3.04 g, 8.0mmol) was dissolved in NMP (15 mL) and added dropwise to the solution of potassium butoxide, during which time the mixture had become warm to the touch. The reaction mixture was placed into a preheated oil bath (120 °C) and stirred for 1.5 h before cooling to room temperature and pouring into an ice/1 N ammonium chloride solution (150 mL). The resulting solid was collected by filtration and dried in a vacuum oven at 60 °C overnight to afford 2.55 g (93%) of 5-chloro-8-methyl-8*H*-imidazo[4,5-*d*]thiazolo[5,4-*b*]pyridine-2-ylbenzamide as an off-white solid. ^{1}H NMR (DMSO-d_6) δ 13.17 (1H, s), 8.49 (1H, s), 8.17 (2H, d, J = 7.3 Hz), 7.70−7.65 (1H, m), 7.60 (2H, t, J = 7.60 Hz), 4.26 (3H, s). MS (ESI) m/z 344, 346 $(M + H)^+$. Purity: 98% (method A, t_R = 2.02 min).

The off-white solid was added portionwise to a hot (85 °C) solution of hydrochloric acid (50 mL), anhydrous ethanol (25 mL), and dioxane (25 mL). The resulting heterogeneous mixture was heated to 100 °C for 16 h, during which time the solution had become homogeneous. The reaction mixture was allowed to cool to room temperature, and then the organics were evaporated under reduced pressure. The remaining precipitate was cooled in an ice bath and carefully neutralized with sodium hydroxide (25% w/v aqueous solution) while keeping the internal temperature below 15 °C. The solid was collected by vacuum filtration and washed with water. The air-dried solid was then triturated in hot acetonitrile and then allowed to cool to room temperature before filtering and allowing to air-dry to afford 1.41 g (67%) of **25** as a light-tan solid. ^{1}H NMR (DMSO-d_6) δ 8.32 (1 H, s), 7.93 (2 H, s), 4.05 (3 H, s). MS (ESI) m/z 240, 242 $(M + H)^+$. Purity: 98% (method A, t_R = 0.69 min), 95% (method B, t_R = 1.08 min).

7-Chloro-4-methyl-2-bromo-4*H*-imidazo[4,5-*d*]thiazolo[5,4-*b*]-pyridine (26). Isoamyl nitrite (5.58 mL, 41.7mmol) was added dropwise over 5 min to a suspension of copper(II) bromide (4.66 g, 20.8mmol) and **25** (5.0 g, 20.8mmol) in anhydrous acteonitrile (150 mL). The reaction mixture was stirred at 65 °C for 16 h before cooling to room temperature and filtering. The solid was slurried in ammonium chloride (10% w/v aqueous solution, 125 mL) and concentrated ammonium hydroxide solution (125 mL) with sonication for 30 min. The suspension was then filtered and dried to afford 4.62 g (73%) **26** as a light-pink solid. ^{1}H NMR (DMSO-d_6) δ 8.61 (1 H, s), 4.25 (3 H, s). HRMS for $C_8H_5N_4Br_1Cl_1S_1$ $(M + H)^+$, calcd: 302.9101. Found: 302.9101. Purity: 97% (method A, t_R = 1.56 min), 97% (method D, t_R = 3.02 min). Anal. Calcd for $C_8H_5N_4Br_1Cl_1S_1$: C, 31.65; H, 1.32; N, 18.45; S, 10.56; Br, 26.32; Cl, 11.67. Found: C, 32.20; H, 1.38; N, 18.57; S, 9.82; Br, 22.33; Cl, 12.60; Cu, <0.01%.

Methyl 7-Chloro-4-methyl-4*H*-imidazo[4,5-*d*]thiazolo[5,4-*b*]-pyridine-2-carboxylate (27). A mixture of **26** (4.00 g, 13.18 mmol), $PdCl_2(PPh_3)_2$ (277 mg, 0.395 mmol), Et_3N (2.75 mL, 19.7 mmol) in CH_3CN (60 mL) and MeOH (60 mL) was stirred under an atmosphere of CO (100 psi) in a bomb at 60 °C. After 24 h, the mixture was cooled to room temperature and depressurized. The solution was concentrated to dryness and triturated with hot ethyl acetate. When the mixture was cooled, the solid was collected by filtration to afford 3.38 g (91%) of **27** as a yellow solid. ^{1}H NMR (DMSO-d_6) δ 8.72 (1 H, s), 4.25 (3 H, s), 3.94 (3H, s). MS (ESI) m/z 283 $(M + H)^+$. Purity: 95% (method A, t_R = 1.60 min)

7-Chloro-4-methyl-4*H*-imidazo[4,5-*d*]thiazolo[5,4-*b*]pyridine-2-carboxylic Acid (28). To a stirring solution of **27** (3.38 g, 12.0 mmol) in THF (700 mL) was slowly added NaOH (1 N, 40 mL). After 40 min, the mixture was concentrated to dryness, 25 mL of cold H_2O was added, the mixture was acidified with 40 mL of 1 N HCl, and the resulting solid was collected by filtration. After the sample was dried under high vacuum, 1.72 g (53%) of **28** was obtained as a colorless solid. ^{1}H NMR (DMSO-d_6) δ 8.62 (1 H, s), 4.19 (3 H, s). MS (ESI) m/z 269 $(M + H)^+$. Purity: 100% (method A, t_R = 1.45 min).

7-Methylamino-4-methyl-4*H*-imidazo[4,5-*d*]thiazolo[5,4-*b*]pyridine-2-carboxylic Acid (29). Starting with **28** (1.71 g) and dividing into 150 mg lots, to each lot was added $MeNH_2$ (33 wt % in EtOH, 1.8 mL) and the suspension heated for 20 min at 150 °C in the microwave reactor. Once cooled to room temperature, the solid was collected by filtration. The combined crude solids were dissolved in a solution of 50 mmol of NH_4OAc in H_2O (50 mL), purified on a C18 column eluted with 50 mmol of NH_4OAc in H_2O solution and gradient with MeOH. Fractions containing product

were combined and concentrated. The resulting solid was dissolved in H_2O and then lyophilized to provide 605 mg (36%) of **29** as a colorless solid. ^{1}H NMR (DMSO-d_6) δ 8.62 (1 H, s), 4.19 (3 H, s), 3.00 (3 H, s). MS (ESI) *m*/*z* 264 $(M + H)^+$. Purity: 95% (method A, $t_R = 1.45$ min).

4-Methyl-7-methylamino-2-methylamido-4*H*-imidazo[4,5-*d*]thiazolo[5,4-*b*]pyridine (30a). To a stirring solution of **29** (32.4 mg, 0.123 mmol) in NMP (0.50 mL) was added $MeNH_2$ (33 wt % in EtOH, 0.20 mL) followed by PyBop (64.1 mg, 0.123 mmol). After 30 min, to the mixture was added AcOH (1 mL), DMF (1 mL). This solution was applied directly onto preparative HPLC to provide 14 mg (36%) of **30a** as a pale-yellow solid. ^{1}H NMR (DMSO-d_6) δ 8.23 (1 H, s), 3.49 (3 H, s), 3.13 (3 H, s), 3.00 (3 H, d, $J = 4.53$ Hz). HRMS for $C_{11}H_{12}O_1N_6S_1$ $(M + H)^+$, calcd: 276.0793. Found: 276.0785. Purity: 95% (method C, $t_R = 8.04$ min), 95% (method D, $t_R = 7.21$ min).

4-Methyl-7-methylamino-2-ethylamido-4*H*-imidazo[4,5-*d*]thiazolo[5,4-*b*]pyridine (30b). 30b was prepared as a pale-yellow solid following the procedure described for **30a**. ^{1}H NMR (DMSO-d_6) δ 8.21 (1 H, s), 3.92 (3 H, s), 3.40 (2 H, q, $J = 4.25$ Hz), 2.97 (3 H, s), 1.20 (3 H, t, $J = 4.25$ Hz). HRMS for $C_{12}H_{14}O_1N_6S_1$ $(M + H)^+$, calcd: 290.0590. Found: 290.0582. Purity: 100% (method C, $t_R = 8.25$ min), 95% (method D, $t_R = 7.54$ min).

4-Methyl-7-methylamino-2-cyclopentylamido-4*H*-imidazo[4,5-*d*]thiazolo[5,4-*b*]pyridine (30c). 30c was prepared as a pale-yellow solid following the procedure described for **30a**. ^{1}H NMR (DMSO-d_6) δ 8.44 (1 H, d, $J = 8.06$ Hz), 8.16 (1 H, s), 7.52 (1 H, d, $J = 4.78$ Hz), 4.24 (3 H, s), 2.98 (3 H, d, $J = 4.78$ Hz), 2.62−2.70 (1 H, m), 2.27−2.36 (2 H, m), 1.48−1.68 (3 H, m), 1.22 (3 H, s). HRMS for $C_{15}H_{19}O_1N_6S_1$ $(M + H)^+$, calcd: 331.133 56. Found: 331.133 73. Purity: 100% (method C, $t_R = 9.86$ min), 95% (method D, $t_R = 9.38$ min).

4-Methyl-7-methylamino-2-diethylamido-4*H*-imidazo[4,5-*d*]thiazolo[5,4-*b*]pyridine (30d). 30d was prepared as a pale-yellow solid following the procedure described for **30a**. ^{1}H NMR (DMSO-d_6) δ 8.12 (1 H, s), 4.12 (3 H, s), 3.06−3.19 (4 H, m), 2.99 (3 H, d, $J = 4.28$ Hz), 1.26−1.40 (3 H, m), 1.17 (3 H, t, $J = 7.05$ Hz). HRMS for $C_{14}H_{19}O_1N_6S_1$ $(M + H)^+$, calcd: 319.133 56. Found: 319.133 48. Purity: 95% (method C, $t_R = 8.19$ min), 95% (method D, $t_R = 8.11$ min).

4-Methyl-7-methylamino-2-thienylamido-4*H*-imidazo[4,5-*d*]thiazolo[5,4-*b*]pyridine (30e). 30e was prepared as a pale-yellow solid following the procedure described for **30a**. ^{1}H NMR (DMSO-d_6) δ 8.19 (1 H, s), 7.54−7.50 (1 H, m), 7.22−7.20 (1 H, m), 7.03−7.01 (1 H, m), 4.63 (2 H, s), 4.15 (3 H, s), 2.95 (3 H, s). HRMS for $C_{15}H_{15}O_1N_6S_2$ $(M + H)^+$, calcd: 358.0671. Found: 356.0668. Purity: 95% (method C, $t_R = 8.15$ min), 95% (method D, $t_R = 7.63$ min).

8-Methyl-2-(4-fluorophenyl)-5-chloro-8*H*-imidazo[4,5-*d*]thiazolo[5,4-*b*]pyridine (31). To a stirred solution of **26** (156.2 mg, 0.50 mmol), 4-fluorophenylboronic acid (170 mg, 1.21 mmol), and $Pd(PPh_3)_4$ (34 mg, 0.0294 mmol) in DME (5 mL) and EtOH (2 mL) was added K_2CO_3 (1 mL, 2 M in H_2O), and then the mixture was heated to reflux. After 1 h, the mixture was cooled to room temperature and the solid collected by filtration and washed with EtOH to afford 61 mg (39%) of **31** as a yellow solid. MS (ESI) *m*/*z* 319 $(M + H)^+$. Purity: 99% (method A, $t_R = 1.45$ min).

***N*-Methyl-2-(4-fluorophenyl)-8-methyl-8*H*-imidazo[4,5-*d*]thiazolo[5,4-*b*]pyridine-5-amine (32a).** A solution of **31** (26.5 mg, 0.0831 mmol) and $MeNH_2$ (33 wt % in EtOH, 0.60 mL) was heated for 60 min at 150 °C in the microwave reactor. The resulting solid was collected by filtration and washed with EtOH to afford 13.6 mg (52%) of **32a** as a pale-yellow solid. ^{1}H NMR (DMSO-d_6) δ 8.14 (1 H, s), 7.99−8.12 (2 H, m), 7.39−7.49 (2 H, m), 4.20 (3 H, s), 2.98 (3 H, d, $J = 4.53$ Hz). HRMS for $C_{15}H_{13}N_5F_1S_1$ $(M + H)^+$, calcd: 314.087 02. Found: 314.086 49. Purity: 100% (method C, $t_R = 11.88$ min), 95% (method D, $t_R = 11.31$ min).

***N*-Ethyl-2-(4-fluorophenyl)-*N*-methyl-8*H*-imidazo[4,5-*d*]thiazolo[5,4-*b*]pyridine-5-amine (32b). 32b** was prepared as a pale-yellow solid following the procedure described for **32a**. ^{1}H NMR (DMSO-d_6) δ 8.16 (1 H, s), 8.02−8.09 (2 H, m), 7.33−7.41 (2 H, m), 7.27 (1 H, t, $J = 5.79$ Hz), 4.21 (3 H, s), 3.48−3.59 (2 H, m), 1.20 (3 H, t, $J = 7.18$ Hz). HRMS for $C_{16}H_{15}N_5F_1S_1$ $(M + H)^+$, calcd: 328.102 67. Found: 328.102 12. Purity: 100% (method C, $t_R = 13.52$ min), 95% (method D, $t_R = 12.41$ min).

8-Methyl-2-(4-fluorophenyl)-8*H*-imidazo[4,5-*d*]thiazolo[5,4-*b*]pyridine-5-amine (32c). 32c was prepared as a pale-yellow solid following the procedure described for **32a**. ^{1}H NMR (DMSO-d_6) δ 8.43 (1 H, s), 8.01−8.21 (2 H, m), 7.41 (2 H, t, $J = 8.81$ Hz), 4.25 (3 H, s). HRMS for $C_{14}H_{11}N_5F_1S_1$ $(M + H)^+$, calcd: 300.0714. Found: 300.0711. Purity: 97.9% (method C, $t_R = 10.47$ min), 94.0% (method D, $t_R = 10.41$ min).

Acetamide, *N*-[2-[[2-(4-Fluorophenyl)-8-methyl-8*H*-imidazo[4,5-*d*]thiazolo[5,4-*b*]pyridine-5-yl]amino]ethyl]-(32d). 32d was prepared as a pale-yellow solid following the procedure described for **32a**. ^{1}H NMR (DMSO-d_6) δ 8.16 (1 H, s), 7.96−8.10 (2 H, m), 7.26−7.47 (2 H, m), 4.19 (3 H, s), 3.48−3.65 (2 H, m), 3.23−3.41 (2 H, m), 1.70 (3 H, s). HRMS for $C_{17}H_{18}O_4N_5F_1S_1$ $(M + H)^+$, calcd: 407.105 81. Found: 407.105 59. Purity: 98.2% (method C, $t_R = 11.23$ min), 91.4% (method D, $t_R = 10.85$ min).

Ethanol, *N*-[2-[[2-(4-Fluorophenyl)-8-methyl-8*H*-imidazo[4,5-*d*]thiazolo[5,4-*b*]pyridine-5-yl]amino]ethyl]-(32e). 32e was prepared as a pale-yellow solid following the procedure described for **32a**. ^{1}H NMR (DMSO-d_6) δ 8.22 (1 H, s), 8.00−8.15 (2 H, m), 7.52−7.64 (1 H, m), 7.24−7.47 (2 H, m), 5.24 (1 H, t, $J = 4.66$ Hz), 4.20 (3 H, s), 3.81 (2 H, d, $J = 6.04$ Hz), 3.65 (2 H, q, $J = 4.95$ Hz), 3.24 (2 H, t, $J = 5.92$ Hz), 3.02−3.12 (2 H, m). HRMS for $C_{18}H_{20}O_1N_6F_1S_1$ $(M + H)^+$, calcd: 387.139 79. Found: 387.139 19. Purity: 98.0% (method C, $t_R = 8.76$ min), 95.0% (method D, $t_R = 10.05$ min).

8*H*-Imidazo[4,5-*d*]thiazolo[5,4-*b*]pyridine-5-amine,2-(4-fluorophenyl)-8-methyl-*N*-[2-(1-piperidinyl)ethyl]-(32f). 32f was prepared as a pale-yellow solid following the procedure described for **32a**. ^{1}H NMR (DMSO-d_6) δ 8.15 (1 H, s), 8.00−8.11 (2 H, m), 7.37 (2 H, t, $J = 8.81$ Hz), 6.96−7.01 (1 H, m), 4.21 (3 H, s), 3.59 (2 H, q, $J = 6.55$ Hz), 2.55 (2 H, t, $J = 6.67$ Hz), 2.35−2.44 (4 H, m), 1.44−1.58 (3 H, m), 1.32−1.43 (3 H, m). HRMS for $C_{21}H_{24}N_6F_1S_1$ $(M + H)^+$, calcd: 411.1762. Found: 411.1760. Purity: 100.0% (method C, $t_R = 10.69$ min), 94.7% (method D, $t_R = 12.57$ min).

***N*-[[3-[8-Methyl-5-chloro-8*H*-imidazo[4,5-*d*]thiazolo[5,4-*b*]pyridine-2-yl]phenyl]methyl]-*tert*-butyl Carbamate (33).** To a stirred solution of **26** (500 mg, 1.65 mmol), 3-(*N*-Boc-aminomethyl)phenylboronic acid (497 mg, 1.98 mmol), and $Pd(PPh_3)_4$ (83 mg, 0.083 mmol) in DME (10 mL) and EtOH (10 mL) was added K_2CO_3 (1.65 mL, 2 M in H_2O, 3.3 mmol), and then the mixture was heated to reflux. After 2 h, the mixture was cooled to room temperature and the solvent evaporated under reduced pressure. The residue was partitioned between water (20 mL) and ethyl acetate (20 mL). The organic layer was dried ($MgSO_4$) and evaporated under reduced pressure before purifying by column chromatography using ethyl acetate as eluent to afford 350 mg (49%) of **33** as a yellow solid. ^{1}H NMR (DMSO-d_6) δ 8.53 (1 H, s), 7.90−8.19 (2 H, m), 7.50−7.66 (2 H, m), 7.40−7.49 (1 H, m), 4.32 (3 H, s), 4.21−4.28 (2 H, m), 1.43 (9 H, s). MS (ESI) *m*/*z* 430, 432 $(M + H)^+$. Purity: 87% (method B, $t_R = 3.40$ min).

***N*-[[3-[8-Methyl-5-methylamino-8*H*-imidazo[4,5-*d*]thiazolo[5,4-*b*]pyridine-2-yl]phenyl]methyl]-*tert*-butyl Carbamate (34).** A solution of **33** (250 mg, 0.58 mmol) and $MeNH_2$ (8 M in EtOH, 4.0 mL, 32mmol) was heated for 10 min at 150 °C in the microwave. The resulting solid was collected by filtration and washed with EtOH to afford 209 mg (85%) of **34** as a pale-yellow solid. MS (ESI) *m*/*z* 425 $(M + H)^+$. Purity: 90% (method B, $t_R = 2.91$ min).

2-[3-(Aminomethyl)phenyl]-*N*,8-dimethyl-8*H*-imidazo[4,5-*d*]thiazolo[5,4-*b*]pyridine-5-amine (35). Hydrochloric acid (4 M in dioxane, 6 mL, 24 mmol) was added in one portion to **34**. The resulting heterogeneous mixture was stirred at room temperature for 20 min before removing the solvent under reduced pressure. The residue was dissolved in water (5 mL) and neutralized with concentrated ammonium hydroxide solution before extracting with chloroform (3 × 15 mL). The combined organics were washed with water (10 mL), then brine (10 mL) and dried ($MgSO_4$) before evaporating under reduced pressure to afford 105 mg (76%) of **35**

as a yellow solid. (DMSO-d_6) δ 8.16 (1 H, s), 8.03 (1 H, d, J = 7.15 Hz), 7.52−7.61 (2 H, m), 7.33 (1 H, d, J = 4.95 Hz), 4.21−4.26 (3 H, s), 4.13 (2 H, s), 3.00 (3 H, d, J = 4.40 Hz). MS (ESI) m/z 325 $(M + H)^+$. Purity: 100% (method B, t_R = 1.70 min).

***N*-[[3-[8-Methyl-5-(methylamino)-8*H*-imidazo[4,5-*d*]thiazolo[5,4-*b*]-pyridine-2-yl]phenyl]methyl]acetamide (36a).** *O*-(7-Azabenzotriazol-1-yl)-*N*,*N*,*N*′,*N*′-tetramethyluronium hexafluorophosphate (126 mg, 0.33mmol) was added in one portion to a stirred mixture of **35** (90 mg, 0.28 mmol) and acetic acid (20 mg, 0.33mmol) in DMF (1 mL). *N*,*N*-Diisopropylethylamine (1.45 mL, 0.832mmol) was then added and the mixture stirred at room temperature for 1 h. Water was added (2 mL) and the precipitated solid was then purified by column chromatography using 10% methanol in dichloromethane as eluent to afford 14.5 mg (12%) of **36a** as a yellow solid. ^{1}H NMR (DMSO-d_6) δ 8.47 (1 H, t, J = 5.79 Hz), 8.16 (1 H, s), 7.86−7.91 (2 H, m), 7.44−7.50 (1 H, m), 7.35 (1 H, d, J = 7.55 Hz), 4.34 (2 H, d, J = 5.79 Hz), 4.22 (3 H, s), 2.99 (3 H, s), 1.90 (3 H, s). HRMS for $C_{18}H_{19}O_1N_6S_1$ $(M + H)^+$, calcd: 367.133 56. Found: 367.132 95. Purity: 95% (method C, t_R = 6.98 min), 95% (method D, t_R = 7.10 min).

***N*-[[3-[8-Methyl-5-(methylamino)-8*H*-imidazo[4,5-*d*]thiazolo[5,4-*b*]-pyridine-2-yl]phenyl]methyl]methanesulfonamide (36b). 36b** was prepared as a pale-yellow solid following the procedure described for **36a**. ^{1}H NMR (DMSO-d_6) δ 8.15 (1 H, s), 7.97 (1 H, s), 7.92 (1 H, d, J = 7.81 Hz), 7.70 (1 H, t, J = 6.30 Hz), 7.51 (1 H, t, J = 7.55 Hz), 7.43−7.47 (1 H, m), 7.33 (1 H, d, J = 4.78 Hz), 4.26 (2 H, d, J = 6.30 Hz), 4.23 (3 H, s), 2.99 (3 H, d, J = 4.53 Hz), 2.91 (3 H, s). HRMS for $C_{17}H_{19}O_2N_6S_2$ $(M + H)^+$, calcd: 403.100 54. Found: 403.099 91. Purity: 96% (method C, t_R = 8.28 min), 95% (method D, t_R = 8.50 min).

***N*-[[3-[8-Methyl-5-(methylamino)-8*H*-imidazo[4,5-*d*]thiazolo[5,4-*b*]-pyridine-2-yl]phenyl]methyl]isoxazole-5-amide (36c). 36c** was prepared as a pale-yellow solid following the procedure described for **36a**. ^{1}H NMR (DMSO-d_6) δ 8.42 (1 H, s), 8.29−8.32 (1 H, m), 7.86 (1 H, s), 7.61−7.68 (2 H, m), 7.36−7.38 (1 H, m), 7.17 (1 H, s), 4.58−4.62 (2 H, m), 4.21 (3 H, s), 3.02 (3 H, s). HRMS for $C_{20}H_{18}O_2N_7S_1$ $(M + H)^+$, calcd: 419.1164. Found: 419.1158. Purity: 100% (method C, t_R = 8.25 min), 95% (method D, t_R = 8.67 min).

***N*-[[3-[8-Methyl-5-(methylamino)-8*H*-imidazo[4,5-*d*]thiazolo[5,4-*b*]-pyridine-2-yl]phenyl]methyl]-1,2,3-thiadiazole-5-amide (36d). 36d** was prepared as a pale-yellow solid following the procedure described for **36a**. ^{1}H NMR (DMSO-d_6) δ 9.71 (1 H, s), 8.14 (1 H, s), 8.01 (1 H, s), 7.84−7.93 (1 H, m), 7.41−7.53 (2 H, m), 4.57−4.66 (2 H, m), 4.17 (3 H, s), 3.00 (3 H, s). HRMS for $C_{19}H_{17}O_1N_8S_2$ $(M + H)^+$, calcd: 437.096 13. Found: 437.095 55. Purity: 98% (method C, t_R = 9.31 min), 95% (method D, t_R = 9.59 min).

***N*-[[2-Fluoro-5-[8-methyl-5-methylamino-8*H*-imidazo[4,5-*d*]-thiazolo[5,4-*b*]pyridine-2-yl]phenyl]methyl]acetamide (37a). 37a** was prepared as a pale-yellow solid following the procedure described for **36a**. ^{1}H NMR (DMSO-d_6) δ 8.40 (1 H, t, J = 5.69 Hz), 8.20 (1 H, s), 7.80−7.89 (2 H, m), 7.35 (1 H, d, J = 7.45 Hz), 4.30 (2 H, d, J = 5.62 Hz), 4.20 (3 H, s), 2.7 (3 H, s), 1.86 (3 H, s). HRMS for $C_{18}H_{18}O_1N_6F_1S_1$ $(M + H)^+$, calcd: 384.1169. Found: 384.1158. Purity: 95% (method C, t_R = 7.24 min), 95% (method D, t_R = 7.56 min).

***N*-[[2-Fluoro-5-[8-methyl-5-methylamino-8*H*-imidazo[4,5-*d*]-thiazolo[5,4-*b*]pyridine-2-yl]phenyl]methyl]methanesulfonamide (37b). 37b** was prepared as a pale-yellow solid following the procedure described for **36a**. ^{1}H NMR (DMSO-d_6) δ 8.38−8.40 (1 H, m), 7.96−7.99 (1 H, m), 7.90 (1 H, s), 7.41−7.45 (1 H, m), 4.24 (2 H, d, J = 6.25 Hz), 4.20 (3 H, s), 2.95 (3 H, d, J = 4.50 Hz), 2.89 (3 H, s). HRMS for $C_{17}H_{18}O_2F_1N_6S_2$ $(M + H)^+$, calcd: 420.0838. Found: 420.0831. Purity: 97% (method C, t_R = 8.54 min), 95% (method D, t_R = 8.67 min).

IKK Enzymatic Activity Assay. Assays measuring the enzyme-catalyzed phosphorylation of GST-IκBα were performed by adding enzyme (IKK-2, typically to a final concentration of 3 μg/mL) at room temperature to solutions of 50 μg/mL GST-IκBα and 20 μM ATP in 25 mM Tris-HCl, pH 7.5, containing 7.5 mM $MgCl_2$, 34 mM sodium phosphate, 3 mM NaCl, 0.6 mM potassium phosphate, 1 mM KCl, 1 mM dithiothreitol, 5% (w/v) glycerol, and 470 μg/mL bovine serum albumin. After 60 min, the kinase reactions were stopped by the addition of EDTA to 33 mM. IκBα phosphorylation was quantitated by competition for binding to an antiphospho-IκBα antibody (SantaCruz Biotechnology no. sc-8404) with fluorescein-labeled phosphopeptide ([FL]-Asp-Asp-Arg-His-Asp-[p]Ser-Gly-Leu-Asp-Ser-Met-Lys-NH2) as measured using fluorescence polarization.

LPS-Induced TNF-α Production in Human Peripheral Blood Mononuclear Cells. Human PBMCs were isolated from whole blood collected from healthy donors. Blood was diluted into RPMI 1640 (Life Technologies) containing 2.5 mM EDTA (Life Technologies) and 10 μg/mL polymyxin (Sigma) and then underlaid with ficoll (Accurate Scientific Co.) and centrifuged at 600*g* for 25 min. The interface was collected, and cells were washed twice and resuspended in RPMI, 10% FBS. Cells are then distributed (200 mL/well) into 96-well tissue culture treated plates (Falcon) at 1×10^6 cells/mL in RPMI, 10% FBS. Test compounds were added to appropriate wells and incubated with cells for 30 min. Cells were then stimulated by the addition of lipopolysaccharide (LPS, BioWhittaker), with a final concentration of 25 ng/mL, and incubated for 6 h at 37 °C, 5% CO_2. The cell supernatants were removed and assayed for TNF-α by ELISA (R&D Systems).

Inhibition of TNF-α Release in Mice. BALB\c female mice, 6−8 weeks of age, were obtained from Harlan Laboratories and maintained ad libitum on water and standard rodent chow (Harlan Teklad). Mice were acclimated to ambient conditions for at least 1 week prior to use. For oral dosing, the compounds were prepared in a solution of 100% poly(ethylene glycol) (MW 300), and a dosing volume of 0.1 mL per mouse was administered on average 4 h prior to LPS injection (0.1 mL of LPS suspended at 10 μg/mL in PBS, administered ip). Blood samples were obtained 90 min after LPS injection. Serum was separated from clotted blood samples by centrifugation (5 min, 5000*g*, room temperature) and analyzed for levels of TNF-α by ELISA assay (R&D Systems) according to the manufacturer's directions. Results are shown as the mean ± SEM of n = 8 mice per treatment group. All procedures involving animals were reviewed and approved by the Institutional Animal Care and Use Committee.

Metabolic Stability in Liver Microsomes. Incubations with mouse, human, and rat liver microsomes (BD Gentest, Woburn, MA) were conducted at 1 mg/mL protein concentration, 3 μM compound in 65 mM phosphate buffer (pH 7.4), and 1 mM β-nicotinamide adenine dinucleotide phosphate (β-NADPH) at 37 °C for 1 h. Aliquots of incubation mixtures (0.2 mL) were taken at 0 and 15 min, and the reaction was quenched with one volume of acetonitrile. The rate of metabolism was calculated on the basis of the fraction of parent disappearance by comparing 15−0 min time points.

Supporting Information Available: X-ray crystallaographic data for compounds **12** and **19**. This material is available free of charge via the Internet at http://pubs.acs.org.

References

(1) (a) Viemann, D. Transcriptional profiling of IKK2/ NF-κB and p38 MAP kinase dependent gene expression in TNF-α stimulated primary human endothelial cells. *Blood* **2004**, *103*, 3365–3373. (b) Neurath, M. F. Role of NF-κB in immune and inflammatory responses in the gut. *Gut* **1998**, *43*, 856–860. (c) Cho, M. L. STAT3 and NF-κB signal pathway is required for IL-23 mediated IL-17 production in spontaneous arthritis animal model IL-1 receptor antagonist-deficient mice. *J. Immunol.* **2006**, *176*, 5652–5661. (d) Zhang, Z. Interleukin-1β and tumor necrosis factor-a upregulate interleukin-23 subunit p19 gene expression in human colonic subepithelial myofibroblasts. *Int. J. Mol. Med.* **2005**, *15*, 79–83. (e) He, K. L.; Ting, A. T. Essential role for IKKg/NEMO in TCR-induced IL-2 expression in Jurkat T cells. *Eur. J. Immunol.* **2003**, *33*, 1917–1924. (f) Snapper, C. M. B cells from p50/NF-κB knockout mice have selective defects in proliferation, differentiation, germ-line CH transcription, and Ig class switching. *J. Immunol.* **1996**, *156*, 183–191. (g) Ruocco, M. G. IκB kinase (IKK)b, but not IKKa, is a critical mediator of osteoclast survival and

is required for inflammation-induced bone loss. *J. Exp. Med.* **2005**, *201*, 1677–1687. (h) Pattoli, M. A. Collagen and aggrecan degradation is blocked in interleukin-1-treated cartlidge explants by an inhibitor of IκB kinase through suppression of metalloproteinase expression. *J. Pharmacol. Exp. Ther.* **2005**, *315*, 382–388.

(2) Whiteside, S. T.; Israel, A. IκB proteins: structure function and regulation. *Semin. Cancer Biol.* **1997**, *8*, 75–82.

(3) Ghosh, S.; Karin, M. Missing pieces in the NF-κB puzzle. *Cell* **2002**, *109*, S81–S96.

(4) Strnad, J.; Burke, J. R. IκB kinase inhibitors for treating autoimmune and inflammatory disorders: potential and challenges. *Trends Pharmacol. Sci.* **2007**, *28*, 142–148.

(5) Saklatvala, J. Glucocorticoids: do we know how they work? *Arthritis Res.* **2002**, *4*, 146–150.

(6) (a) Podolin, P. L. Attenuation of murine collagen-induced arthritis by a novel, potent, selective small molecule inhibitor of IκB kinase 2, TPCA-1 (2-[(aminocarbonyl)amino]-5-(4-fluorophenyl)-3-thiophenecarboxamide), occurs via reduction of proinflammatory cytokines and antigen-induced T cell proliferation. *J. Pharmacol. Exp. Ther.* **2005**, *312*, 373–381. (b) Burke, J. R. BMS-345541 is a highly selective inhibitor of IκB kinase that binds to an allosteric site of the enzyme and blocks NF-κB dependent transcription in mice. *J. Biol. Chem.* **2003**, *278*, 1450–1456. (c) Ziegelbauer, K. A selective novel low-molecular-weight inhibitor of IκB kinase-β (IKK-β) prevents pulmonary inflammation and shows broad anti-inflammatory activity. *Br. J. Pharmacol.* **2005**, *145*, 178–192. (d) Wen, D. A selective small molecule IκB kinase β inhibitor blocks nuclear factor κB-mediated inflammatory responses in human fibroblast-like synovicocytes, chondrocytes, and mast cells. *J. Pharmacol. Exp. Ther.* **2006**, *317*, 989–1001. (e) Belema, M.; Bunker, A.; Nguyen, V. N.; Beaulieu, F.; Ouellet, C.; Qiu, Y.; Zhang, Y.; Martel, A.; Burke, J. R.; McIntyre, K. W.; Pattoli, M. A.; Daloisio, C.; Gillooly, K. M.; Clarke, W. J.; Brassil, P. J.; Zusi, F. C.; Vyas, D. M. Synthesis and structure−activity relationship of imidazo(1,2-a)thieno(3,2-*e*)pyrazines as IKK-β inhibitors. *Bioorg. Med. Chem. Lett.* **2007**, *17*, 4284–4289. (f) Qiu, Y.; Belema, M.; Yang, X.; Zusi, F. C.; Pitts, W. J. Preparation of Pyrazolopurine-Based Tricyclic Compounds for the Treatment of Inflammatory and Immune Diseases. PCT Int. Appl. WO 2004075846, 2004. (g) Beaulieu, F.; Ouellet, C.; Ruediger, E. H.; Belema, M.; Qiu, Y.; Yang, X.; Banville, J.; Burke, J. R.; Gregor, K. R.; MacMaster, J. F.; Martel, A.; McIntyre, K. W.; Pattoli, M. A.; Zusi, F. C.; Vyas, D. Synthesis and biological evaluation of 4-amino derivatives of benzimidazoquinoxaline, benzimidazoquinoline, and benzopyrazoloquinazoline as potent IKK inhibitors. *Bioorg. Med. Chem. Lett.* **2007**, *17*, 1233–1237.

(7) Lam, W. W.; Martin, G. E.; Lynch, V. M.; Simonsen, S. H.; Lindsay, C. M.; Smith, K. Chemistry of the phenoxathiins and isosterically related heterocycles. The synthesis of 2-azathianthrene and selected analogs. *J. Heterocycl. Chem.* **1986**, *23*, 785–791.

(8) Koenigs, E.; Mields, M.; Gurlt, H. Nitrierungsprodukte des γ-aminopyridins. *Chem. Ber.* **1924**, *57*, 1179–1187.

(9) Manitpisitkul, P.; White, R. E. Whatever happened to cassette-dosing pharmacokinetics? *Drug Discovery Today* **2004**, *15*, 652–658.

(10) The Alamar blue assay was conducted according to the protocol described in Zhi-Jun et al. (*J. Immunol. Methods* **1997**, *210*, 25) by using reagents obtained from Biosource International.

JM8015816